Grid cell firing patterns signal environmental novelty by expansion

Caswell Barry[a,b,c,1], Lin Lin Ginzberg[b,d], John O'Keefe[d,e], and Neil Burgess[a,c,1]

UCL Institutes of [a]Cognitive Neuroscience, [b]Behavioural Neuroscience, and [c]Neurology, [d]Department of Cell and Developmental Biology, and [e]Sainsbury-Wellcome Centre for Neural Circuits and Behaviour, University College London, London WC1N 3AR, United Kingdom

Edited by Thomas D. Albright, Salk Institute for Biological Studies, La Jolla, CA, and approved August 31, 2012 (received for review June 11, 2012)

The hippocampal formation plays key roles in representing an animal's location and in detecting environmental novelty to create or update those representations. However, the mechanisms behind this latter function are unclear. Here, we show that environmental novelty causes the spatial firing patterns of grid cells to expand in scale and reduce in regularity, reverting to their familiar scale as the environment becomes familiar. Simultaneously recorded place cell firing fields remapped and showed a smaller, temporary expansion. Grid expansion provides a potential mechanism for novelty signaling and may enhance the formation of new hippocampal representations, whereas the subsequent slow reduction in scale provides a potential familiarity signal.

single unit | spatial memory | hippocampus

Grid cells in the medial entorhinal cortex (mEC) of freely moving rodents exhibit a striking triangular grid-like firing pattern (1). Although the grid patterns are anchored to familiar environmental cues (1, 2), their maintenance in darkness and across different environments (1, 3) suggests that they provide a constant metric for self-motion (1, 3–7). Place cells in hippocampal regions CA1 and CA3 tend to fire in single firing fields (8), coding for self-location within an environment. Place cells create novel representations for new environments ("remapping") (3, 9, 10) providing a neural substrate for memory; they show attractor dynamics (11–13) and long-term plasticity (14), and they become increasingly stable and focal with prolonged experience of an environment (15, 16). In contrast, grid cells are thought to retain their regular spatial structure, scale, and position relative to other grids in novel environments (1, 3), changing only their orientation and spatial offset relative to the environment and showing a brief reduction in spatial stability (1). Grid cells (1, 7, 17), in conjunction with other environmental inputs (6, 18–21), are thought to provide an important input to hippocampal place cells. Conversely, direct and indirect projections from CA1 to the deep layers of the mEC (22, 23) have been proposed as a possibly route by which extrinsic sensory information might reach grids (21), a view supported by developmental and inactivation studies (24–26). Together, these points raise questions about the relationship between entorhinal and hippocampal activity; for example: Does stable grid cell firing co-occur with labile place fields, and what drives place cell remapping?

In experiment 1, we investigated grid cell firing on first exposure to a new environment and as it became increasingly familiar during trials conducted on the same day and then on subsequent days. In experiment 2, we replicated the experiment using different environments, while corecording grid cells and place cells from a second cohort of rats that had received bilateral mEC and hippocampal implants. Together, these experiments showed that grid cell firing patterns were spatially expanded and less regular in novel arenas than in a similarly sized familiar arena. At the same time, place cell firing patterns remapped and increased in size. Repeated exposure to the novel arenas produced an attenuation of these effects.

Results

Experiment 1: Spatial Scale of Grid Cell Firing Expands in Novel Environments. To study how grid cell firing is established and stabilized in a novel environment, we recorded grid cells from the mEC of eight rats as they foraged in geometrically identical 1-m^2 arenas that were placed in distinct locations within the recording room and differed in texture, visual appearance, and odor. The recordings on each day consisted of five 20-min trials: the first and last in a "familiar" arena that had already been explored for at least 100 min and the intervening three trials in a "novel" arena. Cells were recorded on up to 7 consecutive days. If grid cells were still detectable at the end of the first run of 7 days, a different novel environment was introduced and the sequence was repeated (details are provided in *Methods*).

Fig. 1 illustrates the typical response of grid cells during initial exposure to a novel arena. Consistent with previous reports (3), the grid pattern was rotated and shifted relative to the familiar arena; however, in addition, firing fields were larger, spaced farther apart, and less regular. On the first novel trial (trial 2 on day 1), all grids recorded on that day ($n = 22$) expanded in scale (scale measured from the spatial autocorrelogram increased by an average of 13.8 cm or 37.3%; range: 10.5–71.1%; $t_{21} = 10.9$, $P << 0.001$). In general, large grids expanded by a similar absolute amount as small grids. However, too few concurrent recordings of large and small grids existed to quantify the relationship (additional information is provided in Fig. S1). At the same time, in the novel arenas, grids shifted by an average of 16.7 cm relative to the familiar arena (a value that did not differ from that expected by chance; $t_{21} = -0.99$, $P = 0.33$; Fig. S2), compared with 2.3 cm between the repeated familiar trials ($t_{21} = 7.5$, $P << 0.001$), and were rotated apparently randomly (Rayleigh test for circular uniformity, $P = 0.32$); there was no significant correlation between the amount of rotation or shift and the increase in scale. The subsequent two novel arena trials (trials 3 and 4) also showed an increase in grid scale but of reduced magnitude compared with the first novel trial (21.3% expansion in trial 4; ANOVA over trials: $F_{4,105} = 32.09$, $P << 0.001$; trial 4 vs. familiar: $t_{21} = 6.6$, $P << 0.001$; trial 4 vs. trial 2: $t_{21} = -3.8$, $P = 0.001$; Fig. 1*B*). A negative correlation between trial number and size of grid expansion in the novel arena (trials 2–4) indicates that expanded grids continued to reduce in scale during the first 60 min of exposure to the novel arenas (Spearman's $\rho = -0.35$, $P = 0.004$). Over the same period, there was no change in the rotation or shift of the grid firing relative to the familiar arena (Fig. S3).

Consistent with the novelty-related increase in scale measured from the spatial autocorrelogram, individual grid firing fields were larger (mean field area: 1,298 cm^2 in novel vs. 918 cm^2 in familiar; $t_{21} = 3.9$, $P < 0.001$) and also spaced farther apart (mean distance between neighboring fields: 53.2 cm vs. 42.0 cm; $t_{21} = 5.2$, $P << 0.001$). The proportionate increases in field size and spacing were of similar magnitudes to the overall change in grid scale, 20.3% and 26.7%, respectively (the square root of

Author contributions: C.B. and N.B. designed research; C.B. and L.L.G. performed research; C.B. and N.B. analyzed data; and C.B., J.O., and N.B. wrote the paper.

The authors declare no conflict of interest.

This article is a PNAS Direct Submission.

Freely available online through the PNAS open access option.

[1]To whom correspondence may be addressed. E-mail: caswell.barry@ucl.ac.uk or n.burgess@ucl.ac.uk.

This article contains supporting information online at www.pnas.org/lookup/suppl/doi:10.1073/pnas.1209918109/-/DCSupplemental.

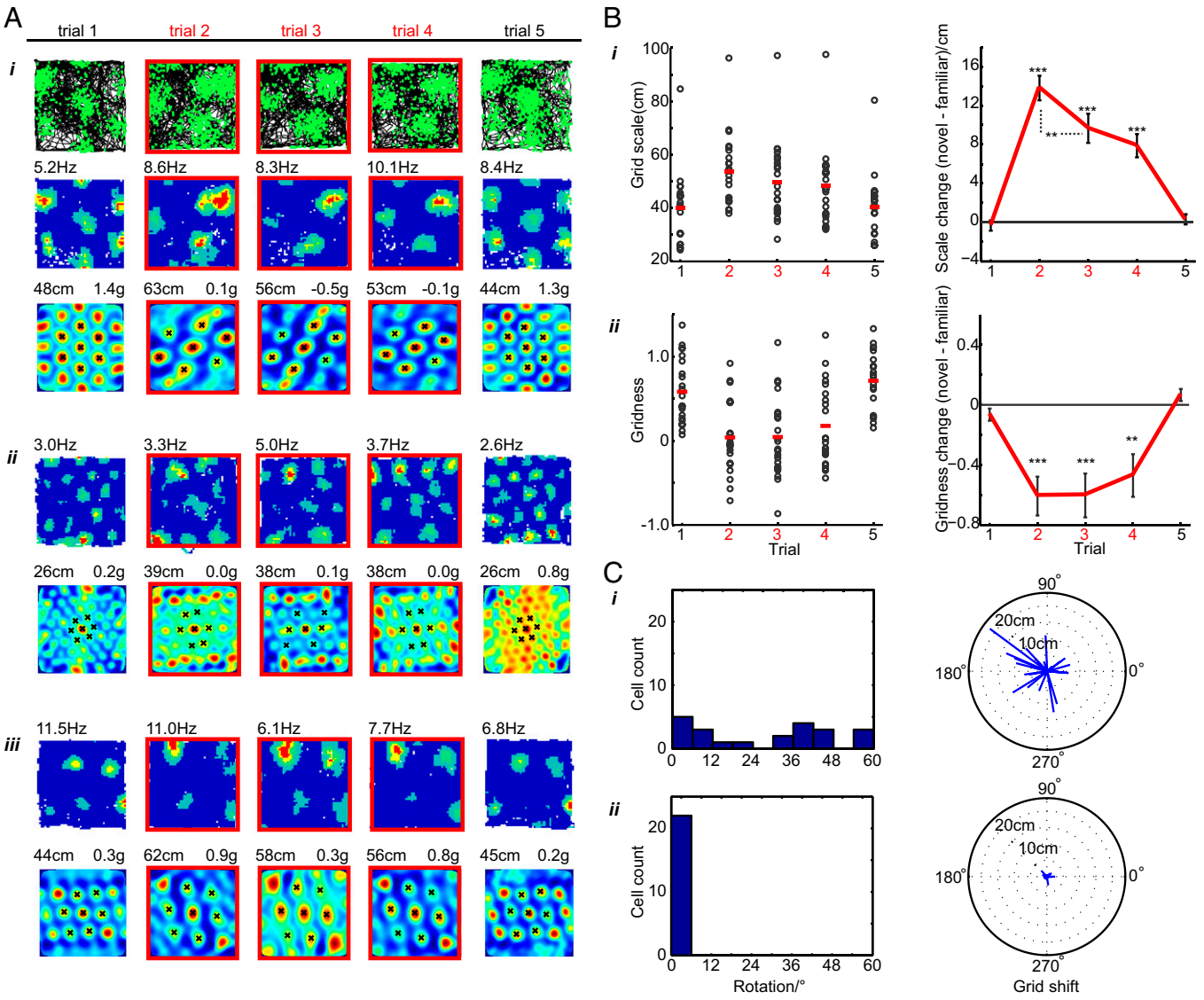

Fig. 1. Grid cell firing patterns expand and become less regular in novel arenas. On the first day of the protocol, trials 1 (*Left*) and 5 (*Right*) were performed in a familiar arena and trials 2–4 were performed in a novel arena (red outline and text). (*A*) Three grid cells (*i–iii*, from different animals) show raw data plots [*Top*; locations of action potentials (green) on the animal's path (black)], firing rate maps [*Middle*; high firing rate (red),low rate (blue), unvisited locations (white), and peak rate (shown above map)], and spatial autocorrelograms (*Bottom*; black crosses show the central peak and six surrounding peaks used to define the grid scale and gridness values (shown above the plot)]. (*B*) All grid cells recorded on day 1 in the novel arena ($n = 22$). (*i*) Grid scale increases in the novel arena (trial 2) and decreases during the subsequent 40 min (trials 3 and 4). Grids return to their original scale in the familiar arena (trial 5; red bars show mean grid scale). (*ii*) Gridness decreases in the novel arena. (*C*) (*i*) Movement of animals between the familiar and novel arenas (trial 1 vs. trial 2) caused grids to rotate (*Left*) and shift (*Right*). (*ii*) Similar comparison between visits to the familiar arena (trial 1 vs. trial 5) indicated that grids maintained the same orientation (*Left*) and offset (*Right*). In all figures, error bars show SEM. $^*P < 0.05$; $^{**}P < 0.01$; $^{***}P < 0.001$ for two-tailed t tests.

field area was used to provide a linear measure of field size), indicating that the relative proportions of the grid pattern in the novel arenas were broadly intact. Grids in novel arenas were also markedly less regular: mean "gridness" [hexagonal regularity of adjacent fields (1)] was reduced to 0.04 on the first novel trial from 0.65 in the familiar arena (ANOVA over trials: $F_{4,105} = 8.08$, $P << 0.001$; trial 2 vs. familiar: $t_{21} = -4.7$, P<0.001) and remained low over the next two novel trials (Fig. 1*B*). Firing fields were less circular in the novel vs. familiar arena (perimeter deviation from circular: 1.58 vs. 1.38; $t_{21} = 3.2$, $P = 0.004$; *Methods*). The reduction in grid regularity was driven partly by distortion (producing a more elliptical rather than circularly symmetrical arrangement of firing), in addition to other factors (Fig. S4). The observed increase in grid scale and reduction in regularity did not vary significantly between directional and nondirectional grid cells or between cells recorded from shallow (II/III) and deep (V/VI) layers (all $P > 0.23$). Neither did we find any effect of the lighting conditions in the novel arenas (dark or light, Table S1; all $P > 0.44$).

Grid Expansion Attenuates Across Days. Novelty-related grid expansion persisted into subsequent days but continued to diminish with experience of the "new" environment. Because the population of grid cells recorded on each day varied between animals, we collapsed data across rats, such that each animal contributed a single value (mean scale in novel minus familiar trials) per day of experience in each novel environment. Grids recorded on day 2 (17 cells from 9 rats), after animals already had 3 trials (60 min) of experience in the novel arena, were still enlarged by an average of 7.5 cm (16.2%; $t_8 = 6.6$, $P < 0.001$), a smaller expansion than on the

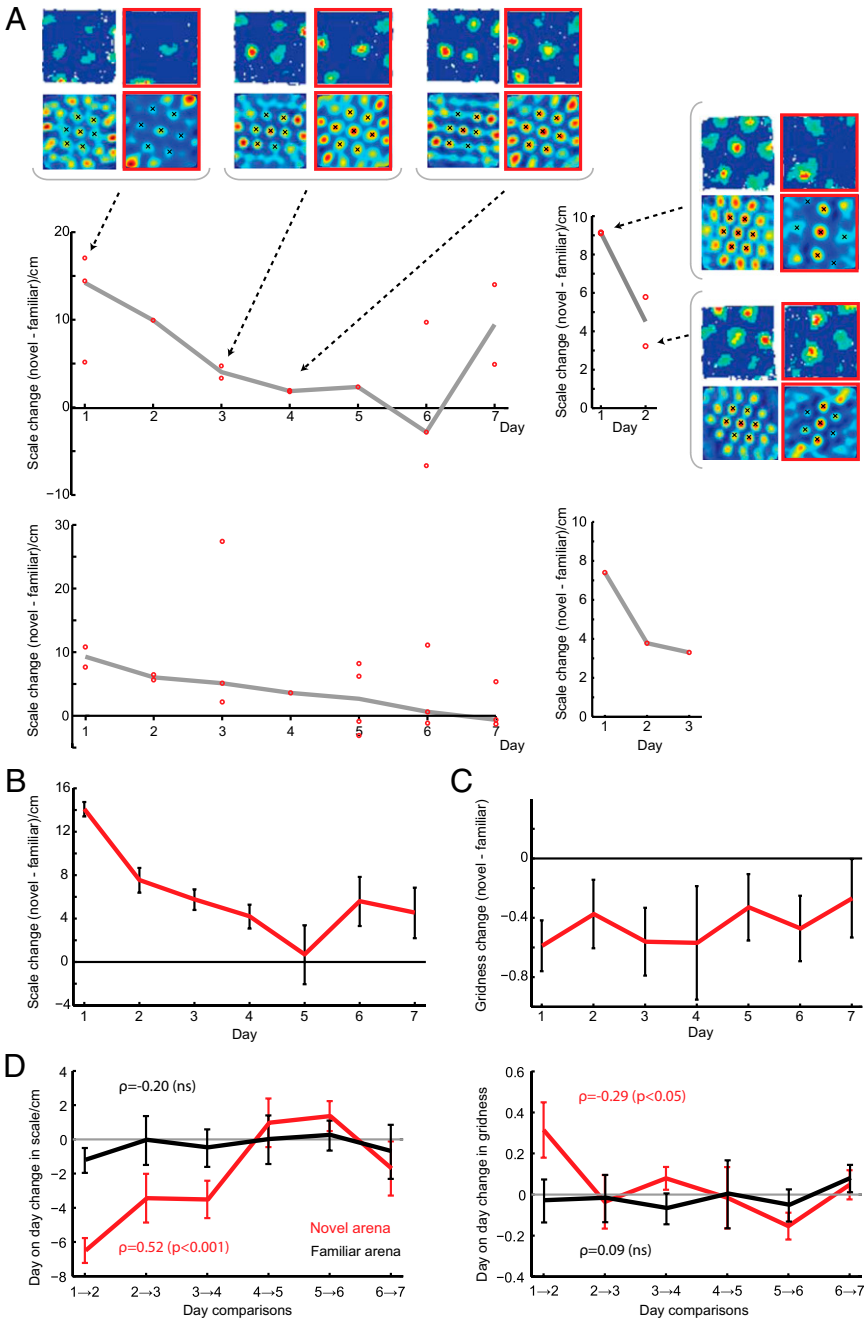

Fig. 2. Novelty-driven grid expansion and irregularity attenuate with experience over days. (*A*) Data from four animals [r1635 (*Upper Left*), r1549 (*Upper Right*), r1625(*Lower Left*), and r1604 (*Lower Right*)] show the difference between novel and familiar grid scales by day (r1635, $n = 14$ cell days; r1549, $n = 4$ cell days; r1625, $n = 18$ cell days; r1604, $n = 3$ cell days; gray line, median change in scale between familiar and novel trials; red circles, data points for individual cells). Arrows indicate rate maps and autocorrelograms for a specific cell recorded over multiple days; in each case, the first rate map corresponds to trial 1 (the first familiar trial of the day) and the second corresponds to trial 2 (the first novel trial of the day; red outline). r1549 and r1604 recordings were truncated after cells were lost. The mean change in grid scale (*B*) and gridness (*C*) between novel and familiar arenas is shown by day. Data shown are the mean over rats from all 34 recording sessions (103 cell days). (*D*) Change in grid scale (*Left*) and gridness (*Right*) for cells recorded on adjacent days for the novel (red) and familiar (black) arenas. The day-to-day reduction in the grid scale in the novel arena attenuates over days, whereas the increase in gridness is focused on days 1–2. Data points show the mean over cells ($n = 52$ cell days), error bars indicate SEM, and Spearman's ρ and the associated *P* value show the correlation between day-to-day change and days of experience.

first day (14.1 cm vs. 7.5 cm; $t_{19} = 5.4$, $P < 0.001$). Grid expansion continued to reduce across days (Spearman's $\rho = -0.72$, $P << 0.001$), and by day 5, grid scale in novel arenas was not distinguishable from that in familiar arenas ($t_4 = 0.24$, $P = 0.25$) (Fig. 2 and Fig. S5). To investigate the time course of reduction, we compared the firing rate maps of individual cells that could be identified on contiguous recording days ($n = 52$ pairs; Fig. 2*D*). Grid scale in the novel arenas reverted toward baseline across the first 3 days (Spearman's $\rho = 0.52$, $P < 0.001$), with no further reduction after the fourth day ($t_6 = 0.68$, $P = 0.52$). In contrast, grid scale in the familiar arena did not change over this period (Spearman's $\rho = 0.20$, $P = 0.17$). A similar but less pronounced return to baseline was seen for grid regularity (Fig. 2*C*); on the second day, grids in the novel arenas still had lower gridness than those in the familiar arena ($t_{16} = -3.2$, $P = 0.006$) and the rate of change in gridness from day to day was reduced in the novel arenas, whereas gridness remained constant in the familiar arena (Fig. 2*D*; novel: Spearman's $\rho = -0.29$, $P = 0.04$; familiar: Spearman's $\rho = 0.09$, $P = 0.54$).

Could behavioral differences between the novel and familiar arenas account for these results? On the first novel trial, animals occupied a similar proportion of the arena as in familiar trials, were stationary for comparable periods of time, and followed paths with comparable tortuosity. However, running speed was slightly lower in the novel arenas (mean: 17.1 cm·s^{-1} vs. 19.6 cm·s^{-1}; $t_{11} = 4.1$, $P < 0.01$), but the difference in speed was not correlated with the change in grid scale (Spearman's $\rho = 0.15$, $P = 0.65$). Nevertheless, to control for this difference, positional data were down-sampled to equate a median running speed of 15 cm·s^{-1} on all trials and firing rate maps were reconstructed. This dataset still showed a large increase in scale and reduction in regularity between novel and familiar trials (mean scale increase = 12.9 cm; $t_{21} = 10.7$, $P << 0.001$; mean gridness reduction = 0.42; $t_{21} = -3.6$, $P = 0.002$; Fig. S6). Rate maps generated from spike-shuffled data were also

analyzed to identify any biases resulting solely from the animals' paths; none were found (details are provided in *SI Methods*). There were no differences in mean firing rate, spatial coherence, or spatial information conveyed by grid cells in the first visit to the novel arena vs. the familiar arena. However, as reported previously (27), we found that theta-modulated grid cells recorded on the first day of the protocol exhibited an inverse relationship between grid scale and the theta-band modulation of their firing rate (intrinsic firing frequency) (after controlling for speed differences, Spearman's $\rho = -0.54$, $P = 0.01$). More specifically, considering the theta-modulated grid cells from all days of the experiment, the reduction in intrinsic firing frequency (between trials 1 and 2) predicted the change in scale of that cell's grid pattern (Fig. S7; Spearman's $\rho = -0.42$, $P = 0.02$).

Experiment 2: Grid Expansion Co-Occurs with Place Cell Remapping. Is grid expansion accompanied by place cell remapping? We simultaneously recorded mEC grid cells and contralateral CA1 place cells from a further seven rats while they experienced a protocol similar to that described above. However, different arenas from those of the first experiment were used, and each was located in a separate room. As with experiment 1, the first visit to a novel arena induced a large increase in grid scale ($n = 16$, average increase = 11.5 cm or 33.9%; $t_{15} = 3.25$, $P < 0.01$) and reduction in grid regularity (mean gridness reduced from 0.96 to 0.31; $t_{15} = -5.33$, $P = 0.001$). Grid expansion was accompanied by an immediate and complete remapping of the rate and location of place cell activity. Spatial correlations between place cells active in both novel and familiar arenas ($n = 32$, mean correlation = 0.243 after accounting for possible rotations of the ensemble) were markedly lower than between visits to the familiar arena ($n = 43$, mean correlation = 0.650; $t_{73} = 7.60$, $P << 0.001$). Similarly, the firing rates of all place cells varied by more between different arenas ($n = 53$, mean novel/familiar rate change of 0.408 vs. 0.267 familiar/familiar; $t_{103} = -2.588$, $P = 0.02$; Fig. 3). Thus, both measures (spatial correlation and rate change) indicated significant remapping, and did so irrespective of the amount of grid expansion in each rat (Spearman's rank correlation, $P > 0.8$ for all).

Similar to the grids, and as indicated previously (15, 16), place fields in the novel arenas were larger than those in the familiar arena (average increase in field area during the first novel trial = 28.8%, a 12.7% increase in diameter; $t_{85} = -2.84$, $P = 0.006$). However, place fields expanded by less than corecorded grids (change in place field diameter vs. grid scale, 12.7% vs. 33.9%; $t_{54} = -2.23$, $P = 0.03$). In the novel arenas, place fields were also less stable than in the familiar arena (intratrial spatial correlation of 0.61 vs. 0.70; $t_{85} = 2.48$, $P = 0.015$) and conveyed less spatial information (0.97 bits/spike vs. 1.26 bits/spike; $t_{85} = 2.34$, $P = 0.02$). Grid expansion also occurred in the following two novel trials (trials 3 and 4, day 1: average increase of 14.6%; $t_{15} = 3.54$, $P < 0.01$ and 16.8%; $t_{15} = 4.10$, $P < 0.01$, respectively), when an increase in place field diameter was also present but did not reach significance on the fourth trial (average increase of 11.3%; $t_{88} = -2.87$, $P < 0.01$ and 7.6%; $t_{88} = -1.84$, $P = 0.07$, respectively; Fig. 3*B*). Thus, place cell firing patterns also showed a novelty-related expansion and subsequent reduction in scale, albeit smaller than in corecorded grid cells.

Discussion

In summary, during an animal's first experience of a new environment and subsequent familiarization with it, grid cell firing patterns undergo marked changes: They initially expand in scale and become irregular and then progressively return to the more regular and significantly smaller spatial scale seen in familiar environments. These effects occur in addition to the temporary reduction in spatial stability of grids noted by Hafting et al. (1) during an animal's first exposure to an environment, an effect we also observed (intratrial spatial correlation of 0.53 in the familiar arena vs. 0.46 in first novel trial; $t_{37} = -2.67$, $P = 0.011$). Concurrently CA1 place cell firing remaps, generating a distinct representation for the new environment, and also exhibits a more subtle expansion-like effect that may relate to changes in place field size and position seen when rats repeatedly run laps on a track (12, 28).

The results described here are distinct from previous reports that parametric changes to the geometry of a familiar arena produce commensurate changes in the spatial firing patterns of grid (2) and place cells (9, 29). These parametric manipulations demonstrate the influence of environmental geometry on established spatial firing patterns but do not cause global remapping. By contrast, our current results concern the effect of environmental novelty on grid and place cell firing, in the absence of any changes in environmental geometry. Indeed, the coherent changes in spatial and temporal frequencies we noted (Fig. S7) suggest an endogenous effect. This inverse relationship between the spatial scale of the grid pattern and the frequency of theta-band modulation of grid cell firing is consistent with several models of grid cell

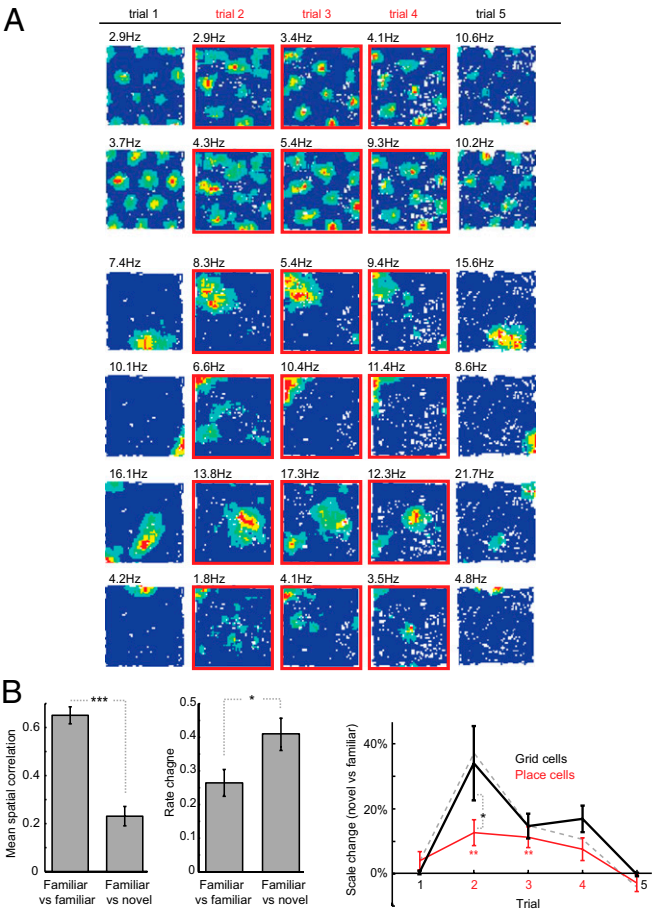

Fig. 3. Grid expansion and irregularity are accompanied by complete remapping of CA1 place cells. (*A*) Firing rate maps for two grid cells and four place cells simultaneously recorded on the first day of the protocol (novel trials outlined in red, data from r1838). (*B*) Moving from the familiar arena to the first trial in the novel arena caused large changes in CA1 place cells' firing location (*Left*, spatial correlation between firing rate maps; correlations were calculated for four 90° rotations of the novel arena relative to familiar arena, and the highest values were reported) and firing rates (*Middle*, absolute difference in mean rate divided by the sum of mean rates), compared with the two familiar trials. (*Right*) Both place field size and grid scale increase during the first novel trial and decrease over subsequent novel trials [red line, percentage increase in place field diameter, defined as square root of increase in field area divided by π, in novel ($n = 40$) vs. familiar ($n = 47$) arenas; black line, percentage increase in grid scale from concurrently recorded grid cells ($n = 16$); and gray dashed line, percentage change in grid field diameter, for comparison]. In all figures, error bars show SEM. $*P < 0.05$; $**P < 0.01$; $***P < 0.001$ for two sample t tests.

formation, including one based on attractors (30) and those based on oscillatory interference (6, 31–33). It seems possible that these temporal changes might be triggered by the release of a neuromodulator, such as ACh, which is implicated in novelty detection (34, 35) and affects both the frequency of theta-band oscillations (36) and the resonant properties of mEC stellate cells (37). The presence of a common modulator is also consistent with the fact that corecorded grid cells tend to expand by similar amounts [considering all grid cells on their first exposure to novelty ($n = 38$), concurrently recorded pairs exhibited a smaller difference in expansion than those recorded at different times, 5.8 cm vs. 10.5 cm; $t_{701} = 2.69$, $P = 0.007$]. In contrast, recordings made from the same animal in different novel arenas did not exhibit similar amounts of expansion, indicating that the degree of modulation is not simply intrinsic to each rat ($t_{208} = 0.18$, $P = 0.86$).

Our results have several implications for the function of grid cells and hippocampal mnemonic function more generally. First, grids do not appear to provide a simple constant spatial metric (1, 7, 21). This does not preclude their involvement in path integration but does indicate a complex dynamic link between grid representations and self-motion. Second, grid expansion and the reduction in regularity produced by environmental novelty may contribute to place cell remapping by providing a temporary mismatch with other hippocampal inputs, such as boundary-related firing, which is unaffected by novelty (18–20). Mismatch would also occur between grid cells expanding by different amounts or around different foci. These short-lived, novelty-related effects exist in addition to grid realignment, a phenomenon that also occurs in response to environmental novelty and is thought to be an important contributor to place cell remapping (3, 38). However, grid realignment does not attenuate with growing familiarity (3), a result we confirmed. As such, the temporary changes in grid firing that we describe would produce an activity pattern that was distinct from the patterns evoked by any familiar environment, would potentially augment the formation of a distinct place cell representation for the new environment (38), and would reduce interference from previously stored representations. Third, the experience-dependent reduction in grid scale may provide a familiarity signal. Such a signal is posited by dual-process models of recognition memory (39, 40) and has previously been identified with regions of the rhinal cortex, including perirhinal and entorhinal cortex (41, 42). In contrast, the complete reorganization and more rapid stabilization of CA1 activity that we observed [as has been noted previously (3, 10, 11, 15), but see also ref. 16], is consistent with a hippocampal role in the recollection of specific spatial configurations or episodes (10, 39, 40). The fact that we observed a spatial correlation greater than 0 between place cells in the familiar and novel arenas partly reflects our conservative method, taking the most correlated ensemble rotation. It is also consistent with previous reports that CA1 representations for different environments are less orthogonal than those found in CA3 (43, 44). Finally, a reduction in grid scale is equivalent to an increase in the resolution with which the grid code represents space (5). It is interesting that we observed an increase in this resolution with experience; whether this reflects the storage of increasing amounts of knowledge or increasingly precise self-localization remains for future work to determine.

Methods

Animals and Surgery. Eight male Lister hooded rats (333–402 g at implantation) each received a single microdrive carrying four tetrodes of twisted 17- to 25-μm heavy polyimide enamael (HML)–coated platinum-iridium wire (90% and 10%, respectively; California Fine Wire) targeted to the right dorsal mEC. Seven additional animals (277–425 g) received two microdrives each, one carrying 12- to 17-μm wire targeted to the mEC and one carrying 17-μm wire targeted to CA1 in the contralateral hemisphere. Wire (12 μm and 17 μm) was platinum-plated to reduced impedance to 200–300 kΩ at 1 kHz. The surgical procedure and housing conditions were the same as those described previously by Barry et al. (2). All work was conducted according to institutional (University College London) and national ethical guidelines in accordance with the UK Animals (Scientific Procedures) Act of 1986.

Recording and Behavioral Training. Training and screening were performed postsurgically after a 1-wk recovery period. An Axona recording system (Axona Ltd.) was used to acquire the single-unit, local field potential (LFP), and positional data. Details of the recording protocol are provided by Barry et al. (2). The position and head direction of the rat were captured using an overhead video camera to record the position of the one or two light-emitting diodes on the animal's head-stage.

All animals were trained to forage for sweetened rice in a 1 × 1-m-square environment, designated as the familiar arena. For the eight rats with a single implant, this arena consisted of a clear Perspex floor and 50-cm-high Perspex walls fronted with gray card (north and south walls) and black ribbed card (east and west walls). The seven rats with double implants were trained in an arena of the same size but constructed from a gray vinyl floor with walls made of Perspex covered by white masking tape. Training consisted of at least five trials of 20 min each, distributed over 3 days. Between trials, the floor of the arena was wiped with a damp cloth to remove feces, urine, and uneaten rice. All subsequent screening took place in this same familiar arena. Once grid cells were detected, a recording session was started. Each recording session consisted of five 20-min trials. The first and last trials always took place in the familiar arena. The intervening three probe trials took place in a novel arena.

For the animals with a single implant, the novel arena, placed within a curtained-off area of the main recording room, was configured in one of two distinct ways, "a" or "b," with both being geometrically identical to the familiar environment (1 × 1-m square with walls 50 cm high) and both being positioned in the same location as each other (i.e., within the curtains). On a given day, and on most consecutive days, each animal would experience the same novel arena (details are provided below). Novel arena a consisted of a black vinyl floor and Perspex walls covered by masking tape. In contrast, novel environment b consisted of a clear Perspex floor scented before each trial with 1 mL of dilute lemon food flavoring (0.1 mL of flavoring to 0.9 mL of water; Supercook) and Perspex walls fronted with white plastic. In all cases, the arena floor was wiped down after each trial.

As long as at least one grid cell was recorded, recording sessions continued in this manner for 7 consecutive days. If no grid cells were present on any day, the electrodes were advanced to find replacements; if none were found within 2 days, the protocol was discontinued. Where possible, spike waveforms and the locations of peak firing were used to follow individual cells between days. If, after successful completion of the 7 day sequence or following discontinuance, grids were present, the protocol was rerun using the same familiar arena but using the other novel arena. To differentiate the two novel arenas further, rats always encountered one of them with the room lights turned off. The sequence of novel arenas and their lighting was counterbalanced across animals, such that of the eight animals, four experienced arena a first, two in the light and two in the dark, and four experienced arena b first, two in the light and two in the dark. Five of the eight animals continued to yield grid cells after the first pass through the experiment and were subsequently exposed to the second novel arena. Because no significant differences were observed between the first and second passes, these 13 blocks of data were analyzed independently. Hence, the dataset includes 13 "day 1" recording sessions; however, one of these sessions did not yield any valid grid cells (Table S1).

A similar protocol was followed for the animals with double implants; again, two possible novel arenas were used, "c" and "d," and these were identically sized to the familiar arena. Arena c was composed of a Perspex floor and Perspex walls fronted with gray card (north and south walls) and black ribbed card (east and west walls). Arena d consisted of black painted hardboard walls and a Perspex floor. However, for these seven animals, the protocol differed in several regards: All three arenas (one familiar and two novel) were located in separate rooms, all trials were run in the light, no odors were applied to the apparatus, and only 4 days of the protocol were run before rerunning with the second novel arena.

Data Analysis. Spike sorting was performed off-line, and 50 × 50 bin (with each bin being 2 × 2 cm) rate maps were produced as described previously (2). Similarly, polar rate maps were constructed using 6° radial bins and were smoothed with a Gaussian kernel ($\sigma = 10°$). LFP was recorded from one or more of the electrodes used for single units, with the signal being amplified 2,000–8,000 times, band-pass filtered at 0.34–125 Hz, and sampled at 250 Hz.

Spatial autocorrelograms of rate maps (1, 4) were used to measure the periodicity, regularity, and orientation of cells with multiple firing fields (2) (further details are provided in *SI Methods*). Similarly, spatial cross-correlograms were used to assess the change in the orientation and translocation ("shift") of grid patterns produced by moving animals between different arenas (3). Rate maps were obtained for each pair of trials that were

compared. To allow for unbiased rotation of the rate maps relative to one another, only their central sections, 1-m-diameter circles, were analyzed. The second rate map was rotated counter-clockwise in increments of 1° by between 0° and 59° using nearest neighbor interpolation. For each rotation the cross-correlogram was calculated in the same way as for autocorrelograms (*SI Methods*) except that $\lambda_1(x,y)$ and $\lambda_2(x,y)$ referred to the unrotated first rate map and the rotated second rate map, respectively. In each case, the peak in the cross-correlogram closest to the origin was found and, ultimately, the rotation that provided the highest peak was selected. The shift of the grid pattern in the second rate map relative to the first was defined as the absolute distance of the central peak from the origin. The rotation of the second rate map relative to the first was taken as the rotation that yielded the autocorrelogram with the highest central peak.

We used two methods to measure the changes in activity exhibited by place cells when animals were moved between the familiar and novel arenas. Changes in the location of spatial firing were assessed by calculating the spatial correlation between rate maps; this was done only for cells that had at least one clear place field in both trials (50 contiguous bins exceeding twice the cell's average firing rate with a mean infield rate ≥1 Hz). Because the novel and familiar arenas were located in different rooms, and thus had no common orienting cues, correlations were calculated for 0°, 90°, 180°, and 270° rotations of the rate maps relative to one another. The rotation that provided the highest mean correlation over concurrently recorded cells was used. Changes in the rate of firing between the familiar and novel arenas were calculated for every place cell and were compared with the change seen between repeated outings in the familiar environment. Rate change was assessed as the absolute difference in mean rate between the two comparator trials divided by the sum of the same mean rates.

Histology. The majority ($n = 7$) of the eight animals with single implants had successful recordings from the dorsolateral extent of the mEC: five had tracks limited to shallow layers (II/III) and two had electrode tracks in the deep layers (V/VI) (Fig. S8). The remaining animal had electrodes placed in the transition zone between the mEC and parasubiculum; as such, it was impossible to say in which of these two structures the recordings had been made. The seven animals with dual implants were confirmed to have recordings from dorsal CA1 and the contralateral dorsolateral mEC (details are provided in *SI Methods*).

ACKNOWLEDGMENTS. We thank K. Jeffery for help with pilot data collection. This study was supported by the Wellcome Trust, a European Union Seventh Framework Programme SPACEBRAIN grant, and the UK Medical Research Council. C.B. received support from the Office of Naval Research via Multidisciplinary University Research Initiative Award N000141010936.

1. Hafting T, Fyhn M, Molden S, Moser MB, Moser EI (2005) Microstructure of a spatial map in the entorhinal cortex. *Nature* 436:801–806.
2. Barry C, Hayman R, Burgess N, Jeffery KJ (2007) Experience-dependent rescaling of entorhinal grids. *Nat Neurosci* 10:682–684.
3. Fyhn M, Hafting T, Treves A, Moser MB, Moser EI (2007) Hippocampal remapping and grid realignment in entorhinal cortex. *Nature* 446:190–194.
4. Sargolini F, et al. (2006) Conjunctive representation of position, direction, and velocity in entorhinal cortex. *Science* 312:758–762.
5. Fiete IR, Burak Y, Brookings T (2008) What grid cells convey about rat location. *J Neurosci* 28:6858–6871.
6. Burgess N, Barry C, O'Keefe J (2007) An oscillatory interference model of grid cell firing. *Hippocampus* 17:801–812.
7. McNaughton BL, Battaglia FP, Jensen O, Moser EI, Moser MB (2006) Path integration and the neural basis of the 'cognitive map' *Nat Rev Neurosci* 7:663–678.
8. Muller RU, Kubie JL, Ranck JB, Jr. (1987) Spatial firing patterns of hippocampal complex-spike cells in a fixed environment. *J Neurosci* 7:1935–1950.
9. Muller RU, Kubie JL (1987) The effects of changes in the environment on the spatial firing of hippocampal complex-spike cells. *J Neurosci* 7:1951–1968.
10. Leutgeb S, et al. (2005) Independent codes for spatial and episodic memory in hippocampal neuronal ensembles. *Science* 309:619–623.
11. Wills TJ, Lever C, Cacucci F, Burgess N, O'Keefe J (2005) Experience-dependent attractors in the hippocampal representation of the local environment. *Science* 308: 873–876.
12. Lee I, Rao G, Knierim JJ (2004) A double dissociation between hippocampal subfields: Differential time course of CA3 and CA1 place cells for processing changed environments. *Neuron* 42:803–815.
13. Nakazawa K, et al. (2002) Requirement for hippocampal CA3 NMDA receptors in associative memory recall. *Science* 297:211–218.
14. Lever C, Wills TJ, Cacucci F, Burgess N, O'Keefe J (2002) Long-term plasticity in hippocampal place-cell representation of environmental geometry. *Nature* 416:90–94.
15. Wilson MA, McNaughton BL (1993) Dynamics of the hippocampal ensemble code for space. *Science* 261:1055–1058.
16. Karlsson MP, Frank LM (2008) Network dynamics underlying the formation of sparse, informative representations in the hippocampus. *J Neurosci* 28:14271–14281.
17. Brun VH, et al. (2002) Place cells and place recognition maintained by direct entorhinal-hippocampal circuitry. *Science* 296:2243–2246.
18. Lever C, Burton S, Jeewajee A, O'Keefe J, Burgess N (2009) Boundary vector cells in the subiculum of the hippocampal formation. *J Neurosci* 29:9771–9777.
19. Savelli F, Yoganarasimha D, Knierim JJ (2008) Influence of boundary removal on the spatial representations of the medial entorhinal cortex. *Hippocampus* 18:1270–1282.
20. Solstad T, Boccara CN, Kropff E, Moser MB, Moser EI (2008) Representation of geometric borders in the entorhinal cortex. *Science* 322:1865–1868.
21. O'Keefe J, Burgess N (2005) Dual phase and rate coding in hippocampal place cells: Theoretical significance and relationship to entorhinal grid cells. *Hippocampus* 15: 853–866.
22. Witter MP, Moser EI (2006) Spatial representation and the architecture of the entorhinal cortex. *Trends Neurosci* 29:671–678.
23. Kloosterman F, van Haeften T, Lopes da Silva FH (2004) Two reentrant pathways in the hippocampal-entorhinal system. *Hippocampus* 14:1026–1039.
24. Wills TJ, Cacucci F, Burgess N, O'Keefe J (2010) Development of the hippocampal cognitive map in preweanling rats. *Science* 328:1573–1576.
25. Langston RF, et al. (2010) Development of the spatial representation system in the rat. *Science* 328:1576–1580.
26. Hafting T, Fyhn M, Bonnevie T, Moser MB, Moser EI (2008) Hippocampus-independent phase precession in entorhinal grid cells. *Nature* 453:1248–1252.
27. Jeewajee A, Barry C, O'Keefe J, Burgess N (2008) Grid cells and theta as oscillatory interference: Electrophysiological data from freely moving rats. *Hippocampus* 18: 1175–1185.
28. Mehta MR, Barnes CA, McNaughton BL (1997) Experience-dependent, asymmetric expansion of hippocampal place fields. *Proc Natl Acad Sci USA* 94:8918–8921.
29. O'Keefe J, Burgess N (1996) Geometric determinants of the place fields of hippocampal neurons. *Nature* 381:425–428.
30. Navratilova Z, Giocomo LM, Fellous JM, Hasselmo ME, McNaughton BL (2011) Phase precession and variable spatial scaling in a periodic attractor map model of medial entorhinal grid cells with realistic after-spike dynamics. *Hippocampus* 22:772–789.
31. Welday AC, Shlifer IG, Bloom ML, Zhang K, Blair HT (2011) Cosine directional tuning of theta cell burst frequencies: Evidence for spatial coding by oscillatory interference. *J Neurosci* 31:16157–16176.
32. Hasselmo ME (2008) Grid cell mechanisms and function: Contributions of entorhinal persistent spiking and phase resetting. *Hippocampus* 18:1213–1229.
33. Giocomo LM, Zilli EA, Fransén E, Hasselmo ME (2007) Temporal frequency of subthreshold oscillations scales with entorhinal grid cell field spacing. *Science* 315: 1719–1722.
34. Hasselmo ME, Wyble BP, Wallenstein GV (1996) Encoding and retrieval of episodic memories: Role of cholinergic and GABAergic modulation in the hippocampus. *Hippocampus* 6:693–708.
35. Thiel CM, Huston JP, Schwarting RK (1998) Hippocampal acetylcholine and habituation learning. *Neuroscience* 85:1253–1262.
36. Buzsáki G (2002) Theta oscillations in the hippocampus. *Neuron* 33:325–340.
37. Heys JG, Giocomo LM, Hasselmo ME (2010) Cholinergic modulation of the resonance properties of stellate cells in layer II of medial entorhinal cortex. *J Neurophysiol* 104: 258–270.
38. Monaco JD, Abbott LF (2011) Modular realignment of entorhinal grid cell activity as a basis for hippocampal remapping. *J Neurosci* 31:9414–9425.
39. Eichenbaum H, Otto T, Cohen NJ (1994) Two functional components of the hippocampal memory system. *Behav Brain Res* 17:449–517.
40. Brown MW, Aggleton JP (2001) Recognition memory: What are the roles of the perirhinal cortex and hippocampus? *Nat Rev Neurosci* 2:51–61.
41. Xiang J-Z, Brown MW (1998) Differential neuronal encoding of novelty familiarity and recency in regions of the anterior temporal lobe. *Neuropharmacology* 37: 657–676.
42. Leonard BW, Amaral DG, Squire LR, Zola-Morgan S (1995) Transient memory impairment in monkeys with bilateral lesions of the entorhinal cortex. *J Neurosci* 15: 5637–5659.
43. Leutgeb S, Leutgeb JK, Treves A, Moser MB, Moser EI (2004) Distinct ensemble codes in hippocampal areas CA3 and CA1. *Science* 305:1295–1298.
44. Leutgeb JK, et al. (2005) Progressive transformation of hippocampal neuronal representations in "morphed" environments. *Neuron* 48:168–169.